EFFECT OF PARTIAL HEATING, COOLING, HEATER LOCATION AND ASPECT RATIO ON NATURAL CONVECTION IN A RECTANGULAR ENCLOSURE

R.Y. Sakr
Mech. Eng. Dept., Faculty of Eng. (Shoubra), Zagzig University

ABSTRACT

The flow and heat transfer in a rectangular enclosure with different heater and cooler sizes, heater location and aspect ratio were studied numerically. Two dimensional mathematical model was developed based on solving the partial differential equations for the conservation of mass, momentum, and energy. A laminar flow is to be considered in the present model. Finite element technique was utilized for the model formulation. The heating element was an isothermal strip located in one, otherwise insulated vertical wall. In the opposing vertical wall, the isothermal cooling element was fitted and the rest of the wall was kept insulated and the upper and lower surfaces were insulated. Computations were carried out at $Pr = 0.7$, $Ra \leq 10^7$. A complete range of cooler and heater sizes and heater location was studied. The computed model results were verified through the comparison with those available in the literature. The computed rates of heat transfer and flow field provide a guidance for locating the heater and cooler. New correlations relating Nusselt number to the dimensionless size of heater and cooler and aspect ratio were obtained.

1. INTRODUCTION

Natural convection in enclosures has received increasing attention in recent years. This attention is due to the wide range of applications in which natural convection plays an important role. Such applications are solar collectors, building air conditioning, insulation with double pane windows, cooling of electronic equipment, crystal growth, nuclear reactor design and furnace design. Natural convection problems also have been a subject of interest for the studies whose objective was to develop numerical methods for the solution of the partial differential equations. Problems involving natural convection can broadly be divided into two categories: Enclosures heated from side and enclosures heated form below [1].

Natural convection in enclosures is a complex phenomenon. For a confined natural convection, a boundary layer forms near the walls. The region exterior to it forms a circulating core. Since the core region is encircled by the boundary layer, the boundary layer can not be considered to be independent of the core. Therefore, the boundary layer and the core are closely coupled to each other. This coupling constitutes the main difficulty in obtaining the analytic solutions. Hence internal natural convection phenomena are most investigated either by numerical or experimental technique.

Novak and Nowak [2] analyzed numerically the natural convection in a rectangular enclosure to investigate the effect of the distance between the vertical walls on the heat transfer rate. As a result of their study, they proposed an optimum gap width for double pane windows. Vertical cavities with isothermal vertical walls have also been studied by Eckert and Carlson [3], Tabarrok and Lin [4] and Korpela et al [5]. Natural convection in a differentially heated corner region has been studied by November and Nansteel [6]. Such circumstances are found when the solar radiation passing through a large window is incident on the floor which receives the radiation and attains a temperature relatively greater than that of the cold window surfaces. Ozoe et al [7] studied experimentally the effect of the inclination angle on the rate of heat transfer in a rectangular enclosure heated from below and cooled from above. Their study was

Engng. Res. Jour., Vol. 59, pp.85- 100, OCTOBER 1998
Helwan University, Faculty of Engng, Matatia Cairo

carried out for different aspect ratios. Sernas and Lee [8] investigated interferometrically the heat transfer rates inside rectangular air enclosures of different aspect ratios less than one (shallow cavities). The enclosures were composed of isothermal vertical walls and the top and the bottom wall were either isothermal or insulated with low thermal conductivity polyurethane foam rubber. Also, the problem of shallow cavities was modeled by Bejan and Tien [9]. Merker and Leal [10] who considered the problem of natural convection in a shallow annular cavity with differentially heated inner and outer walls.

In most of the studies published in literature, the whole vertical wall was considered to be isothermal or the whole wall was exposed to a constant heat flux. However, in many engineering applications, heating and or cooling takes place over a narrow segment of the vertical walls. In such cases, the size and location of the heater and cooler plays an important role on the fluid flow and heat transfer mechanisms. Hence, optimum heater and cooler size and their locations should be determined for better utilization of such system. Chu et al [11] studied the effect of the heater size and location on the rate of heat transfer. In their study one of the vertical walls was partially heated while the whole opposite vertical wall was kept at lower temperature. Also, Yucel and Turkoglu [12] studied numerically the effect of heater and cooler size on the flow and heat transfer in a square enclosure. Their treatment of the velocity-pressure coupling is based on SIMPLE algorithm. Their results showed that the effect of heater size is not in agreement with those of [11]. None of the previous studies provided engineers and designers with precise correlations for the heater and cooler size effect on the heat transfer rate. So, the present work is carried out to achieve this purpose.

In the present study, a square enclosure was considered to study the flow and heat transfer in natural convection problem. An isothermal heating element was located on the left vertical wall and an isothermal cooling element was placed on the right vertical wall. Top and bottom walls were assumed to be insulated. The effect of both heater and cooler sizes on the flow field and heat transfer rate were investigated. Also, the effects of the heater location and the aspect ratio were analyzed.

2. *MATHEMATICAL FORMULATION*

The proposed system is a rectangular enclosure of geometry and coordinates system as shown in Fig. (1). The height of enclosure is denoted by H, and the width by L. The enclosure is heated partially from the left side with a heater length l_h starting from the bottom, where its centerline is located at a distance D from the bottom of the enclosure. Also the enclosure is cooled partially from the right side with a cooler length of l_c starting from the top. The dimensions of the enclosure, heater and cooler normal to the plane of the diagram, are assumed to be long. Hence, the problem can be considered as a two dimensional problem. At time $t > 0$, constant but different temperatures are suddenly imposed on both the heating and cooling vertical elements and maintained until steady state conditions are reached. The steady state equations of the fluid motion are written as:

Mass conservation

$$\frac{\partial u}{\partial x}+\frac{\partial v}{\partial y}=0 \qquad (1)$$

Momentum conservation

$$u\frac{\partial u}{\partial x}+v\frac{\partial u}{\partial y}=-\frac{1}{\rho}\frac{\partial p}{\partial x}+\nu\left(\frac{\partial^2 u}{\partial x^2}+\frac{\partial^2 u}{\partial y^2}\right) \qquad (2\text{-a})$$

$$u\frac{\partial v}{\partial x}+v\frac{\partial v}{\partial y}=g\beta\,(T-T_\infty)-\frac{1}{\rho}\frac{\partial p}{\partial y}+\nu\left(\frac{\partial^2 v}{\partial x^2}+\frac{\partial^2 v}{\partial y^2}\right) \qquad (2\text{-b})$$

Energy conservation

$$\rho c\left(u\frac{\partial T}{\partial x}+v\frac{\partial T}{\partial y}\right)=k\left(\frac{\partial^2 T}{\partial x^2}+\frac{\partial^2 T}{\partial y^2}\right) \tag{3}$$

By eliminating the pressure between the two momentum equations (2-a) and (2-b) and introducing the definitions of vorticity and stream function as in the following equations:

$$\omega=\left(\frac{\partial v}{\partial x}-\frac{\partial u}{\partial y}\right) \tag{4}$$

$$u=\frac{\partial \psi}{\partial y}\ ,\quad v=-\frac{\partial \psi}{\partial x} \tag{5}$$

Using suitable reference values for length, velocity, stream function, and vorticity the dimensionless temperature, vorticity and stream function that govern the natural convection problem can be written in normalized (ξ-η) plane as follows:

$$A_r\left(\frac{\partial \Psi}{\partial \eta}\frac{\partial \Theta}{\partial \xi}-\frac{\partial \Psi}{\partial \xi}\frac{\partial \Theta}{\partial \eta}\right)=A_r^2\left(\frac{\partial^2 \Theta}{\partial \xi^2}\right)+\frac{\partial^2 \Theta}{\partial \eta^2} \tag{6}$$

$$A_r\left(\frac{\partial \Psi}{\partial \eta}\frac{\partial \Omega}{\partial \xi}-\frac{\partial \Psi}{\partial \xi}\frac{\partial \Omega}{\partial \eta}\right)=Ra\,Pr\,A_r\frac{\partial \Theta}{\partial \xi}+Pr\left(A_r^2\frac{\partial^2 \Omega}{\partial \xi^2}+\frac{\partial^2 \Omega}{\partial \eta^2}\right) \tag{7}$$

$$-\Omega=A_r^2\frac{\partial^2 \Psi}{\partial \xi^2}+\frac{\partial^2 \Psi}{\partial \eta^2} \tag{8}$$

a-Initial Conditions:

at $\tau>0\ ,\ 0\le\xi\le1.0\ ,\ 0\le\eta\le1.0$ $\quad\Theta(\xi,\eta)=\Theta_a=0.5$ (average between 1.0,0.0) (9-a)

$\Omega(\xi,\eta)=0.0$ (9-b)

$\psi(\xi,\eta)=0.0$ (9-c)

b- Boundary Conditions:

1- Temperature boundary conditions

at $\xi=0,\quad 0\le\eta\le(l_H/H)$ $\quad\Theta=\Theta_H=1.0$ (10-a)

at $\xi=0,\quad (l_H/H)<\eta\le1.0$ $\quad\dfrac{\partial\Theta}{\partial\xi}=0.0$ (10-b)

at $\xi=1.0\ ,\quad 0\le\eta\le(1-l_c/H)$ $\quad\dfrac{\partial\Theta}{\partial\xi}=0.0$ (10-c)

$\xi=1.0\quad (1-l_c/H)<\eta\le1.0$ $\quad\Theta=\Theta_c=0.0$ (10-d)

at $\eta=0$ and $\eta=1.0,\quad 0\le\xi\le1.0$ $\quad\dfrac{\partial\Theta}{\partial\eta}=0.0$ (10-e)

2- Stream function boundary conditions

At the solid wall boundaries the values of velocity components u and v are zero; so

$$\frac{\partial\Psi}{\partial\eta}=0.0 \tag{11-a}$$

$$\frac{\partial\Psi}{\partial\xi}=0.0 \tag{11-b}$$

The above two equations mean that the solid wall has a constant value of the stream function which is usually assigned a zero value, so the stream function on the solid boundaries is;

$$\Psi_w = 0.0 \tag{12}$$

3- Vorticity boundary conditions

Since the definition of the vorticity can be given by Eq. (8), the no slip boundary condition becomes;

$$\omega = -\frac{d^2\psi}{(dn)^2} \tag{13}$$

Equation (13) can be approximated by using finite difference formulas and expressing it in terms of dimensionless variables as follows:

$$\Omega_w = \frac{2(\Psi_{w+1} - \Psi_w)}{(\Delta N)^2} \tag{14}$$

where; w refers to the nodal value at the no slip wall.
w+1 refers to the adjacent interior node.
ΔN is the dimensionless distance separating this node pair.

Equations (6), (7) and (8) are solved with the relevant boundary conditions given by Eqs. (10), (12) and (14) to determine the temperature, vorticity and stream function distributions. The local Nusselt number is calculated from the temperature distribution as:

$$Nu_y = -\frac{H}{\Delta T}\left(\frac{\partial T}{\partial x}\right)_{x=0} \tag{15}$$

Form the local Nusselt number, the average Nusselt number can be calculated by:

$$\overline{Nu} = \frac{1}{l_H}\int_0^{l_H} Nu_y dy \tag{16}$$

3-NUMERICAL SOLUTION AND FINITE ELEMENT FORMULATION

The system of equations (6), (7) and (8) forms a set of quasilinear elliptic equations. So, the solutions of the system of equations for Ψ, Ω and Θ will be continuous in the domain. Hence, the system of equations was solved in the following iterative procedure. Initially the stream function is assumed to have a zero value every where and Eq. (6) is then solved as a linear equation for Θ. This solution describes the temperature distribution for the pure conduction case. This temperature distribution and the associated stream function field are then substituted into Eq. (7) from which Ω is obtained. Finally the obtained votricity distribution is used in Eq. (8) and an improved value of Ψ is obtained. The cycle of iteration is repeated until the values of Ψ for two consecutive calculations are within $\pm$ 0.02%.

The system of equations is solved using the Galerkin based finite element method [13,14,15]. The objective of the finite element is to reduce the system of governing equations into a discretized set of algebric equations. The procedure begins with the division of the continuum region of interest into a number of simply shaped regions called elements.

The Finite Element Formulation

The temperature, vorticity and the stream function in an element as shown in Fig. (2) can be represented in terms of nodal temperature, vorticity and stream function respectively by simple polynomials:

$$\Theta^e = \sum_{m=1}^{3} N_m \Theta_m \tag{17-a}$$

$$\Omega^e = \sum_{m=1}^{3} N_m \Omega_m \tag{17-b}$$

$$\Psi^e = \sum_{m=1}^{3} N_m \Psi_m \tag{17-c}$$

where;

$$N_1 = \frac{1}{2A}\,(a_1 + b_1 \xi + c_1 \eta) \tag{18-a}$$

$$N_2 = \frac{1}{2A}\,(a_2 + b_2 \xi + c_2 \eta) \tag{18-b}$$

$$N_3 = \frac{1}{2A}\,(a_3 + b_3 \xi + c_3 \eta) \tag{18-c}$$

A = area of the triangle 123

where;

$a_1 = \xi_2 \eta_3 - \xi_3 \eta_2$ $\quad a_2 = \xi_3 \eta_1 - \xi_1 \eta_3$ $\quad a_3 = \xi_1 \eta_2 - \xi_2 \eta_1$

$b_1 = \eta_2 - \eta_3$ $\quad b_2 = \eta_3 - \eta_1$ $\quad b_3 = \eta_1 - \eta_2$

$c_1 = \xi_3 - \xi_2$ $\quad c_2 = \xi_1 - \xi_3$ $\quad c_3 = \xi_2 - \xi_1$

The interpolation functions $[N_1, N_2, N_3]$ in Eqs. (18) are derived from an assumption of linear variation of temperature, vorticity and stream function in the element. The approximate expressions of the system variables are substituted into the governing equations (6)-(8) and the global errors are minimized using the above interpolation functions N_i (i = 1, 2, 3) as weighting functions. The solution of Eqs. (6), (7) and (8) that satisfies the boundary conditions given by Eqs. (10), (12) and (14), can be written after weighted integration over the domain G^e and the application of Green's theorem, in the equivalent matrix form as:

$$[K_1]\{\Theta\} = \{F_1\} \tag{19-a}$$

$$[K_2]\{\Omega\} = \{F_2\} \tag{19-b}$$

$$[K_3]\{\Psi\} = \{F_3\} \tag{19-c}$$

where,

$[K_1] = [K_I] + [K_{II}]$

$$[K_I] = \sum_{e=1}^{E} \int_{G^e} \left(A_e \frac{\partial [N]^T}{\partial \xi}\frac{\partial [N]}{\partial \xi} + \frac{\partial [N]^T}{\partial \eta}\frac{\partial [N]}{\partial \eta}\right) dG$$

$$[K_{II}] = \sum_{e=1}^{E} \int_{G^e} A_e \left(\Psi_\xi \frac{\partial [N]}{\partial \eta} - \Psi_\eta \frac{\partial [N]}{\partial \xi}\right) dG$$

$$\{F_1\} = \sum_{e=1}^{E} \int_{\Gamma^e} [N]^T \frac{\partial T}{\partial n}\, d\Gamma$$

where;

E = total number of elements, G bounded domain, Γ domain boundary,

$$\Psi_\xi = \frac{\partial \Psi}{\partial \xi}, \quad \Psi_\eta = \frac{\partial \Psi}{\partial \eta}$$

Similarly, $[K_2]$, $[K_3]$, $\{F_2\}$and $\{F_3\}$ can be written in the same manner. Equations (19a-c) give three sets of linear equations which have been solved by Gauss elimination method. The finite element formulation and the resulting linear equations were solved through a computer program written here in FORTRAN code.

4- MODEL VALIDATION

To check the consistency and reliability of the present analysis, the same conditions employed by Eckert and Carlson [16] was used in the predictions. Figure (3) shows the obtained results compared with experimental results of Eckert and Carlson. The maximum deviation of the present predictions as can be seen is within 8 %. The average Nusselt number is correlated by a formula of the form of ($Nu = a\ Gr^b$) for air as a working fluid. The numerical predictions of Berkovesky & Polevikov [18] and Balaji and Venkateshan [19] carried out at Eckert and Carlson condition are also plotted in Fig. (3) as can be seen, the agreement between the present predictions and them is fair. Table (1) shows the value of a and b pertaining to the studies in Figure (3).

Table 1: Values of a and b from studies indicated in Fig. (3):

Source	a	b
Eckert & Carlson [16]	0.119	0.30
Han [17]	0.0782	0.359
Berkovsky & Polevikov [18]	0.15	0.29
Balaji & Venkateshan [19]	0.13	0.305
Present work	0.154	0.278

5- RESULTS AND DISCUSSIONS

All the results presented in this paper are for Pr = 0.7. The effect of heater and cooler sizes, heater location and aspect ratio on the flow and heat transfer characteristics are demonstrated. These computations were carried out for different Rayleigh numbers. Either heating or cooling was from vertical sides, while the top and bottom surfaces were insulated.

5.1 Effect of Partial Heating and Cooling

To investigate the effect of heater size on the flow and heat transfer, the cooler size is kept constant and the heater size was varied to take values of $l_h/H = 0.25, 0.5, 0.75$ and 1.0 respectively. The heating element was starting from the bottom of the left side and the cooling element was starting from the top of the right side. For the case of dimensionless cooler size, $l_c/H = 1.0$, the stream lines, isovorticity lines and isotherms for $Ra = 2x10^4$ are illustrated in Figs (4)-(6) respectively. From these figures, it is noticed that the density of isotherms is higher near the heater, hence higher heat transfer rate is achieved. Also, the isovorticity lines core is directed towards the heater where the shape of streamlines does not greatly changed by the heater size.

To analyze the effects of the cooler size on the flow and heat transfer, computations were performed by taking the heater size constant and varying the cooler size l_c/H to take

values of 0.25, 0.5, 0.75 and 1.0 respectively. For the case of $l_h/H=1.0$, stream lines, isovorticity lines and isotherms are shown in Figs. (7)-(9).

The variation of the average Nusselt number with heater and cooler size is illustrated in Figs.(10a-d) for different Rayleigh numbers. These figures show that the average Nusselt number increases with the increase of the cooler size. Also, from the figures it is shown that the average Nusselt number increases with the decrease of the heater size. The effect of the cooler size on the rate of heat transfer for different Rayleigh numbers for a dimensionless heater size $l_h/H = 0.5$ is depicted in Fig. (11). From the figure, it is noticed that the average Nusselt number increases with the increase of cooler size and Rayleigh number. From the present predictions in Figs. (10) and (11), the average Nusselt number can be given as a function of heater and cooler size for different Rayleigh numbers by:

$$Nu = 0.192\ Ra^{0.295}\ (l_h/H)^{-0.37}\ (l_c/H)^{0.42}\ ,\ 10^6 \geq Ra \geq 2\times10^4 \qquad (22)$$

From the above correlation, it is concluded that the average Nusselt number increases with the increase of the cooler size, Rayleigh number and with the decrease of the heater size

5.2 Effect of Rayleigh Number

The effect of Rayleigh number on the fluid flow and heat transfer characteristics is shown in Figs. (12-14). These figures illustrate the stream function, vorticity and temperature contours for different values of Rayleigh number and for complete heater and cooler size. From these figures, it is noticed that as Rayleigh number increases the stream function and vorticity increases. Also, multi-vorticity cells and more thermal stratification are observed for higher Rayleigh numbers.

5.3 Effect of Heater Location

The dependence of the average Nusselt number on the heater location for a heater size l_h/H of 0.2 in a square enclosure for different Rayleigh numbers is illustrated in Figure (15). It is noticed that the average Nusselt number has a maximum value when the heater is located at the bottom of the enclosure and then decreases slightly upto heater location D/H =0.4 and it dreceases sharply to reach a minimum value at a heater location D/H=0.9. So, it can be concluded that the heater location for high heat transfer rate shifts toward the bottom of the enclosure and the heater location D/H having a value of about 0.4 was the limit for high rate of heat transfer in this study where the hot air layer can travel upward and enhances the convection circulation.

5.4 Effect of Aspect Ratio

The effect of aspect ratio has been investigated for a range from 0.1 to 3.0. Figure (16), shows the variation of the average Nusselt number with the aspect ratio for different Rayleigh numbers. It is noticed from the figure that the average Nusselt number increases rapidly with the increase of the aspect ratio till it becomes unity and then the rate of increase in the average Nusselt number is small with the increase of the aspect ratio above unity.

6- CONCLUSIONS

In view of what has been introduced the following conclusions can be drawn;

1- A two dimensional numerical model is devised to simulate the flow and heat transfer in natural convection problems in enclosures with partially or completely heating from one side and partially or completely cooling from the opposite side.

2- A new correlation relating Nusselt number with Rayleigh number, heater and cooler size is obtained.
3- For the side heating condition, the average Nusselt number increases with the increase with the aspect ratio in the range used in this work.
4- For a dimensionless heater size l_h/H= 0.2 and dimensionless cooler size l_c/H =1.0, the average Nusselt number is found to have a maximum value at the bottom location and minimum value at the top location and the dimensionless heater location (D/H) having a value of 0.4 was the limit of high heat transfer rate.

REFERENCES

1- Mills, A.F., Heat Transfer, IRWIN, 1992.
2- Novak, M. H., Howak, E. S., " Natural Convection Heat Transfer in Slender Window Cavities", ASME J. of Heat Transfer, Vol. 115, pp. 476-479, 1993.
3- Eckert, E.R.G. and Carlson, W.O., "Natural Convection in an Air Layer Enclosed Between Two Vertical Plates of Different Temperatures", Int. J. of Heat and Mass Transfer, Vol. 2, pp. 106-120, 1961.
4- Tabarrok, B., and Lin,C.R., "Finite Element Analysis of Free Convection Flows", Int. J. of Heat and Mass Transfer, Vol. 20, pp. 945-952, 1977.
5- Korpela, S. A., Lee, Y. and Drummond, J. E., "Heat Transfer Through a Double Pane Window", ASME J. of Heat Transfer, Vol. 104, pp. 539-544, 1982.
6- November, M. and Nansteel, M. W., " Natural Convection in Rectangular Enclosures Heated from Below and Cooled Along Side", Int. J. of Heat and Mass Transfer, Vol. 30, pp. 2433-2440, 1987.
7- Ozoe, H., Sayama, H. and Churchill, S.W., "Natural Convection in an Inclined Rectangular Channel at Various Aspect Ratios and Angles- Experimental Measurements" , Int. J. of Heat and Mass Transfer, Vol. 18, pp. 1425-1431, 1975.
8- Sernas, V. and Lee, E. I., "Heat Transfer in Air Enclosures of Aspect Ratio Less Than One", J. of Heat Transfer, Vol. 103, pp. 617-622, 1981.
9- Bejan, A. and Ten, C.L., "Natural Convection Heat Transfer in a Horizontal Cavity with Different End Temperature ", ASME J. of Heat Transfer, Vol. 100, pp. 641-647, 1978.
10-Merker, G. P. and Leal, L. G., "Natural Convection in a Shallow Annular Cavity", Int. J. of Heat and Mass Transfer, Vol. 23, pp. 677-686, 1980.
11-Chu, H.H.S., Churchill, S.W. and Patterson, C. V. S., " The Effect of Heater Size, Location, Aspect Ratio and Boundary Conditions on Two-Dimensional Laminar Natural Convection in Rectangular Channel", J. of Heat Transfer, pp. 194-201, 1976.
12-Yucel, N. and Turkoglu, H., "Natural Convection in Rectangular Enclosures with Partial Heating and cooling", Warme-und Stoffubertragung, Vol. 29, pp. 471-478, Springer-Verlag 1994.
13-Rao, S. S., The Finite Element Methods in Engineering, Pergamon Press, 1982.
14-Baker, A. J., Finite Element Computational Fluid Mechanics, Hemisphere Publishing Corporation, New York, 1983.
15-Pepper, D.W., and Heinrich, J.C., The Finite Element Method- Basic Concepts and Applications, Hemisphere Publishing Corporation, 1992.
16- Eckert, E.R. G. and Carlson, W.O. "Natural Convection in an Air Layer", Int. J. Heat Mass Transfer, Vol. 2 , pp. 106-120, 1961.
17- Han, T.J. "Numerical Solutions for an Isolated Votex in a Slot and Free Convection Across a Square Cavity", M.A.Sc. Thesis, University of Toronto, 1967.

18- Berkovsky, B. M. and Polevikov, V.K. "Numerical Study of Problems of High Intensive Free Convection. In Turbulent Buoyant Flow and Convection, D.B. Spalding and N. Afghan (eds.), Vol. 2, Hemisphere, Washington, 443-445, 1977.

19- Balaji, C. and Venkateshan, S.P. "Interaction of Surface Radiation with Free Convection in a Square Cavity", Int. J. Heat and Fluid Flow, Vol. 14, No. 3, Sept. 1993.

NOMENCLATURE

a_1, b_1, c_1	coefficient in Eqs. (18)
A	element area
A_r	aspect ratio; H/L
c	specific heat
D	heater center location apart from the x-axis
dn	distance between two adjacent nodes in the normal direction to the wall boundary
E	total number of elements
$\{F_1\}$, $\{F_2\}$,..	force vectors given by Eqs. (19)
g	gravitational acceleration
G	domain
Gr	Grashof number $g\beta\Delta TH^3)/\nu^2$
H	height of the cavity
k	thermal conductivity
$[K_1]$, $[K_2]$,...	stiffness matrix given by Eqs. (19)
L	length of the cavity
l_C, l_H	cooler and heater length
N_1, N_2, ..	interpolation function
$\overline{Nu}$	average Nusselt number
Nu_y	local Nusselt number
p	pressure
Pr	Prandtl number (ν/α)
Ra	Rayleigh number $(g\beta\Delta TH^3)/\nu\,\alpha$
Ra_L	Rayleigh number $(g\beta\Delta TL^3)/\nu\,\alpha$
t	time
T	temperature
u	velocity component in x-direction
U	dimensionless velocity component in x-direction; u/U_o
U_o	reference velocity; α/H
v	velocity component in y-direction
V	dimensionless velocity component in y-direction; v/U_o
x	horizontal axis
y	vertical axis

Greek letters

α	thermal diffusivity
β	coefficient of thermal expansion
Θ	dimensionless temperature; $(T-T_C)/(T_H-T_C)$
Γ	boundary
ρ	density
ω	vorticity
ξ	dimensionless horizontal axis; x/L
η	dimensionless vertical axis; y/H
τ	dimensionless time; $\alpha t/H^2$
ν	kinematic viscosity
ΔN	dimensionless distance between two adjacent nodes in the normal direction to the wall boundary
ΔT	temperature difference, $T_H - T_C$
Ψ	dimensionless stream function; ψ/α
Ω	dimensionless vorticity; $\omega H/U_o$

Superscripts

e	element level
T	transpose
—	average value

Subscripts

c	cooler, cold
H	heater, hot
m	= 1, 2, 3
o	reference
w	wall

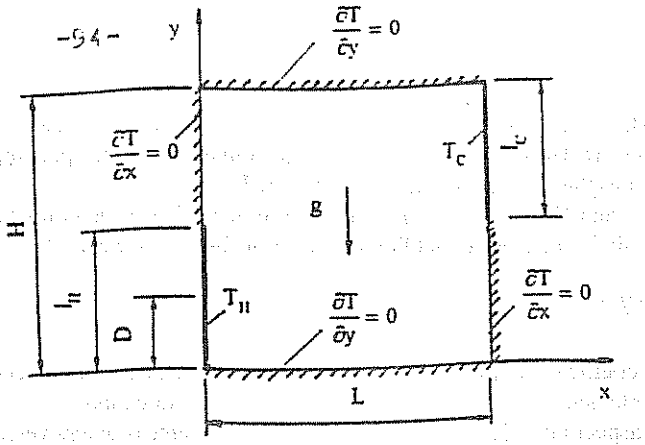

Fig. (1) Geometry, coordinates system and thermal boundary conditions

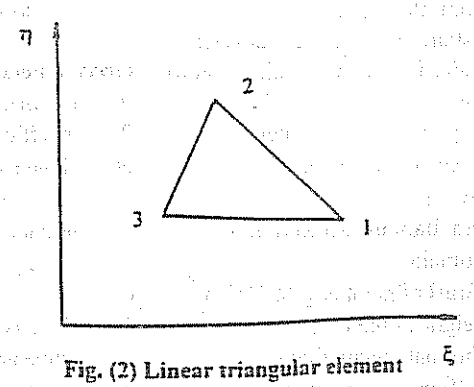

Fig. (2) Linear triangular element

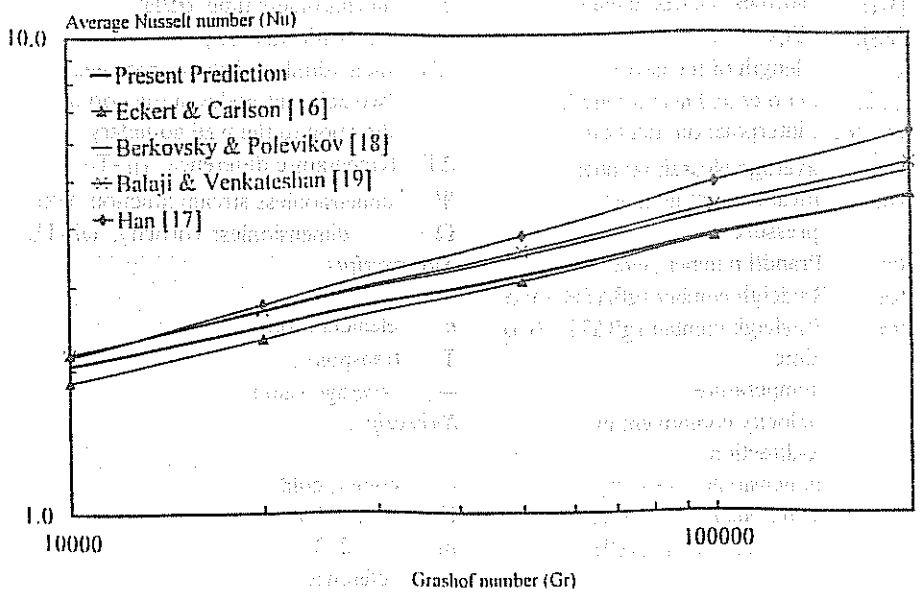

Fig. (3) Comparison between the present prediction and the available previous data

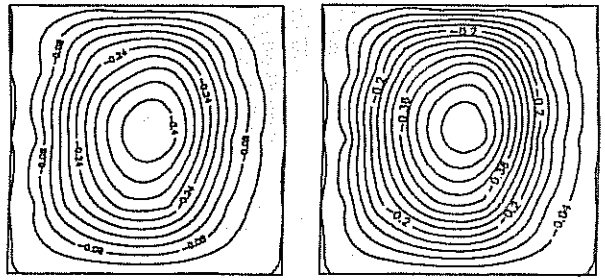

Fig. (4.a-d) Streamline contours ($Ra = 2x10^4$, $l_C/H=1.0$)
(a) $l_H/H = 0.25$ (b) $l_H/H = 0.50$
(c) $l_H/H = 0.75$ (d) $l_H/H = 1.00$

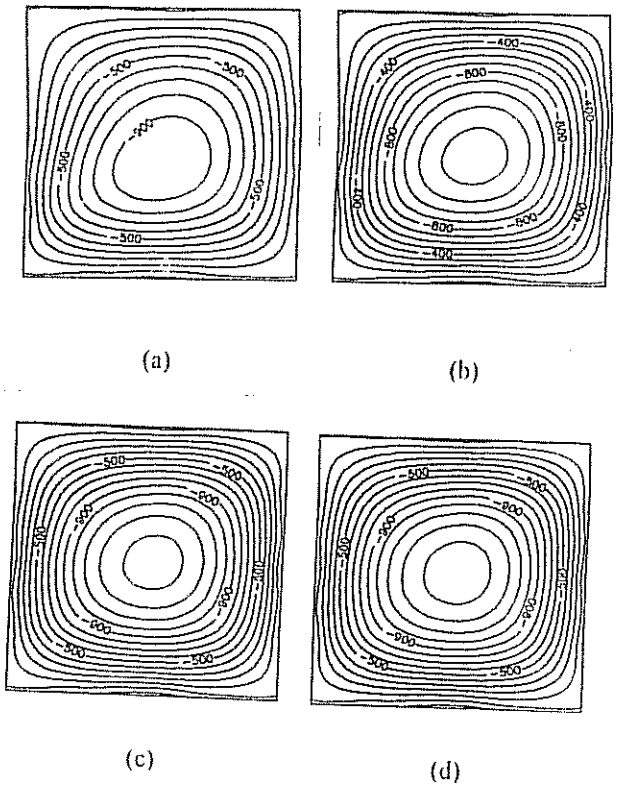

Fig. (5.a-d) Isovorticity line contours ($Ra = 2x10^4$, $l_C/H=1.0$)
(a) $l_H/H = 0.25$ (b) $l_H/H = 0.50$
(c) $l_H/H = 0.75$ (d) $l_H/H = 1.00$

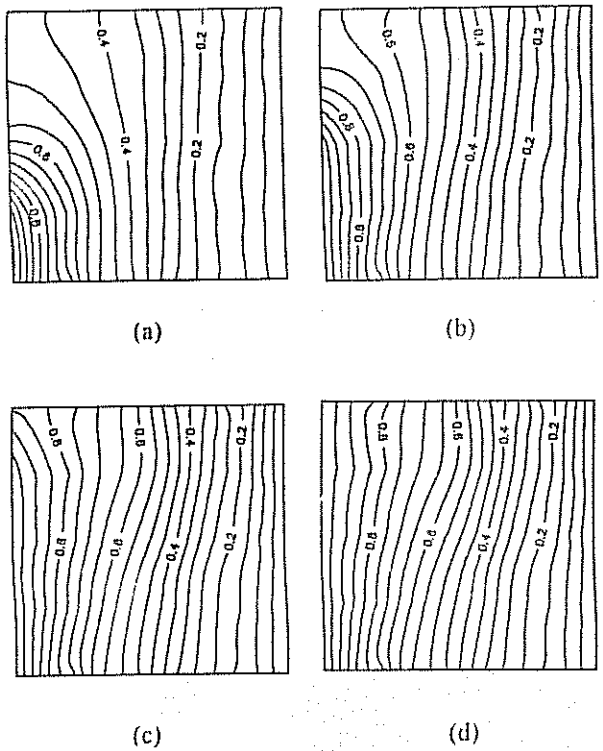

(a) (b)

(c) (d)

Fig. (6.a-d) Isotherm contours ($Ra = 2x10^4$, $l_C/H=1.0$)
(a) $l_H/H = 0.25$ (b) $l_H/H = 0.50$
(c) $l_H/H = 0.75$ (d) $l_H/H = 1.00$

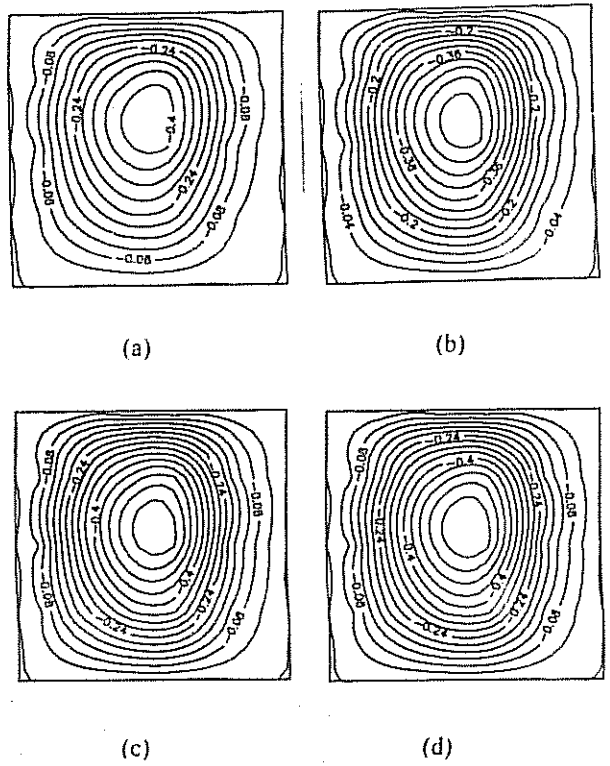

(a) (b)

(c) (d)

Fig. (7.a-d) Streamline contours ($Ra = 2x10^4$, $l_H/H=1.0$)
(a) $l_C/H = 0.25$ (b) $l_C/H = 0.50$
(c) $l_C/H = 0.75$ (d) $l_C/H = 1.00$

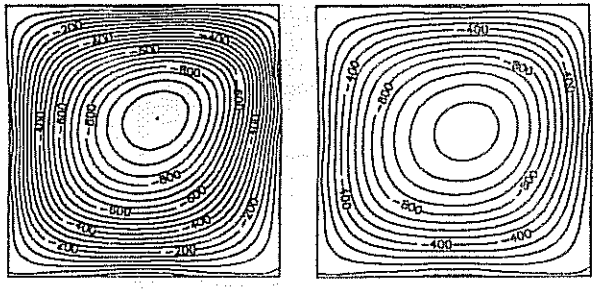

(a) (b)

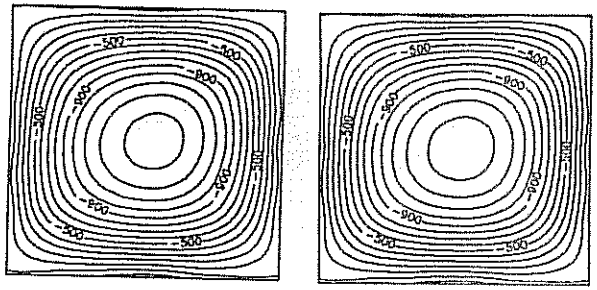

(c) (d)

Fig. (8.a-d) Isovorticity line contours ($Ra = 2x10^4$, $l_H/H=1.0$)
(a) $l_C/H = 0.25$ (b) $l_C/H = 0.50$
(c) $l_C/H = 0.75$ (d) $l_C/H = 1.00$

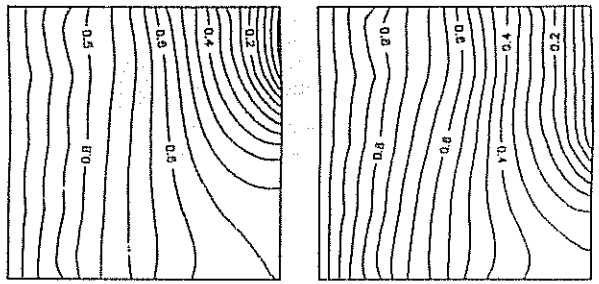

(a) (b)

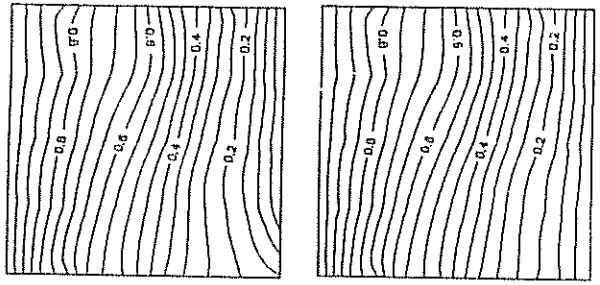

(c) (d)

Fig. (9.a-d) Isotherm contours ($Ra = 2x10^4$, $l_H/H=1.0$)
(a) $l_C/H = 0.25$ (b) $l_C/H = 0.50$
(c) $l_C/H = 0.75$ (d) $l_C/H = 1.00$

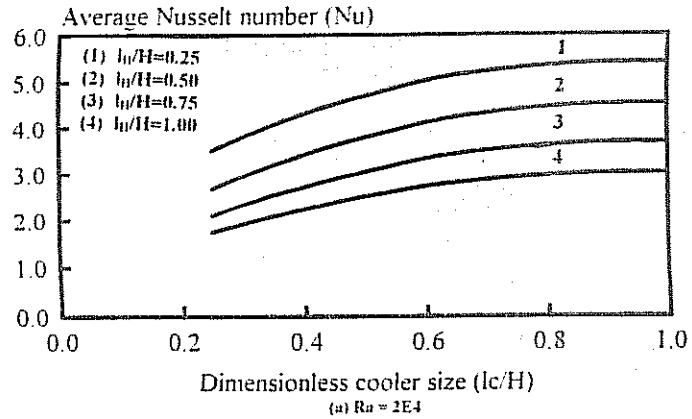

(a) Ra = 2E4

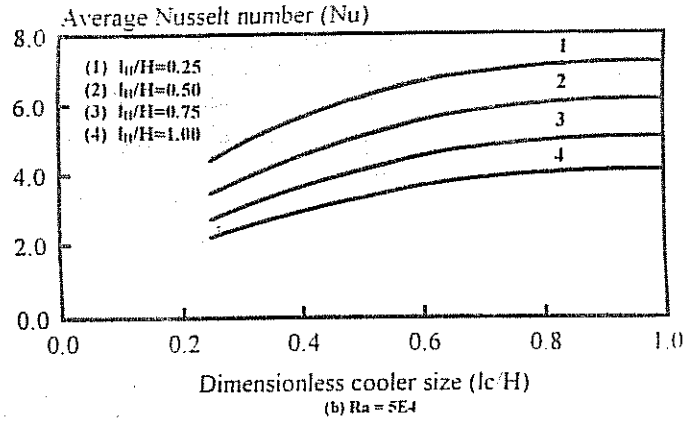

(b) Ra = 5E4

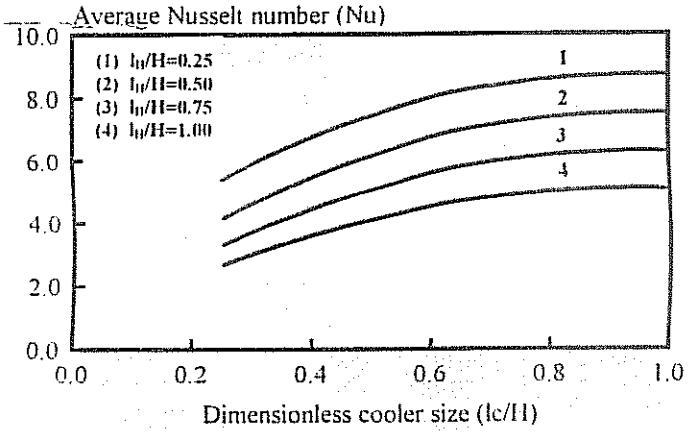

(c) Ra = 1E5

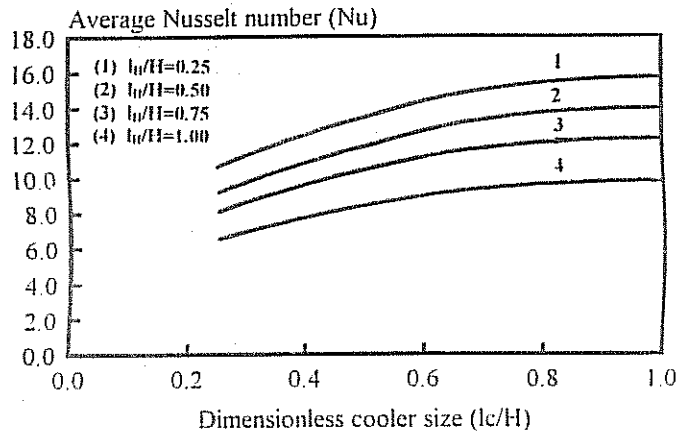

(d) Ra = 1E6

Fig. (10.a-d) Variation of the average Nusselt number with heater and cooler size

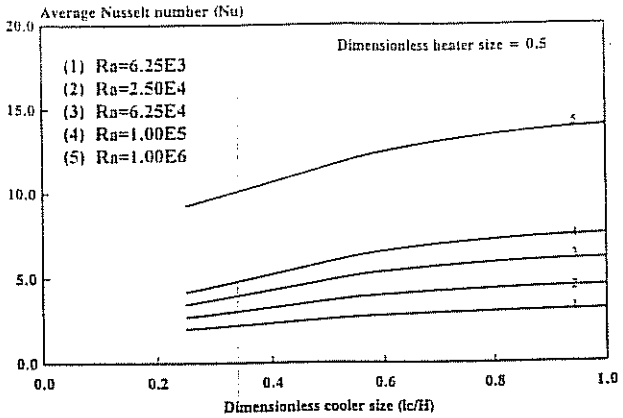

Fig. (11) Variation of the average Nusselt number with the cooler size and Rayleigh number

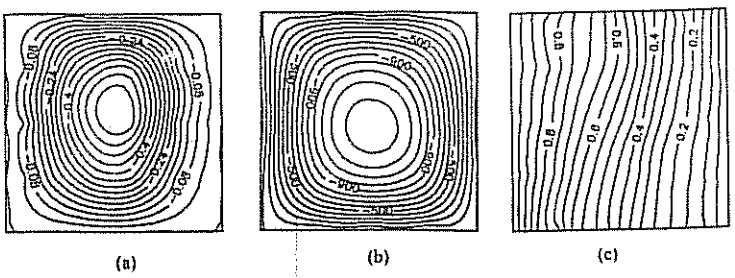

Fig. (12.a-c) Streamline, vorticity and isothermal contours ($Ra = 2x10^4$, $l_H/H = 1.00$, $l_C/H=1.0$)

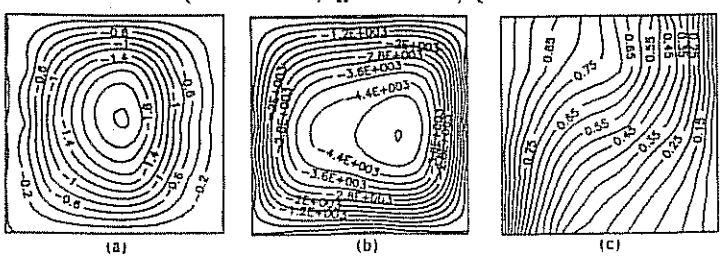

Fig. (13.a-c) Streamline, vorticity and isothermal contours ($Ra = 10^5$, $l_H/H = 1.00$, $l_C/H=1.0$)

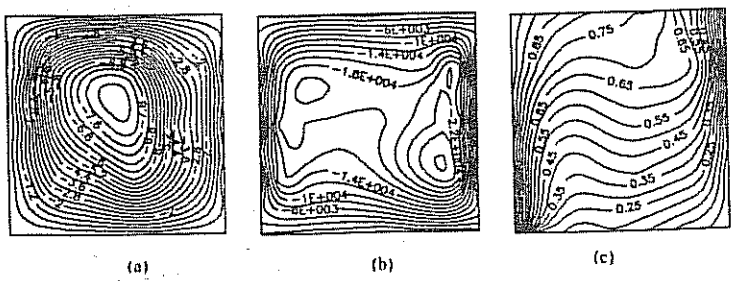

Fig. (14.a-c) Streamline, vorticity and isothermal contours ($Ra = 10^6$, $l_H/H = 1.00$, $l_C/H=1.0$)

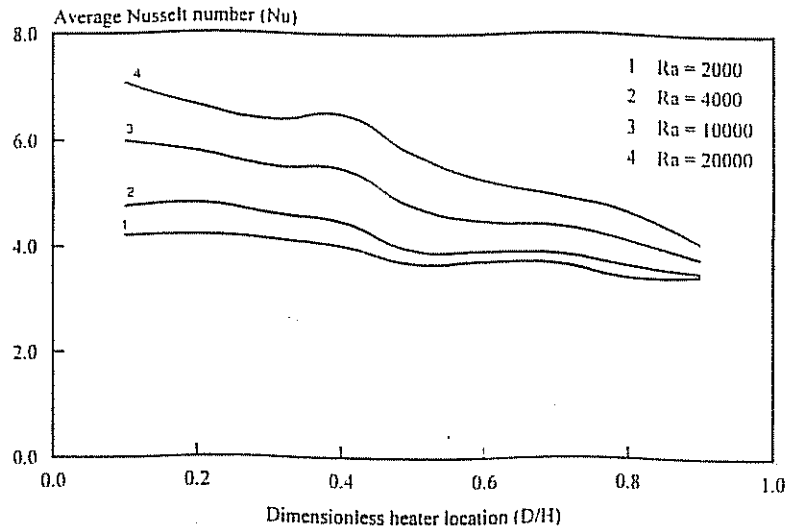

Fig. (15) Variation of the average Nusselt number with the heater location for different Rayleigh numbers

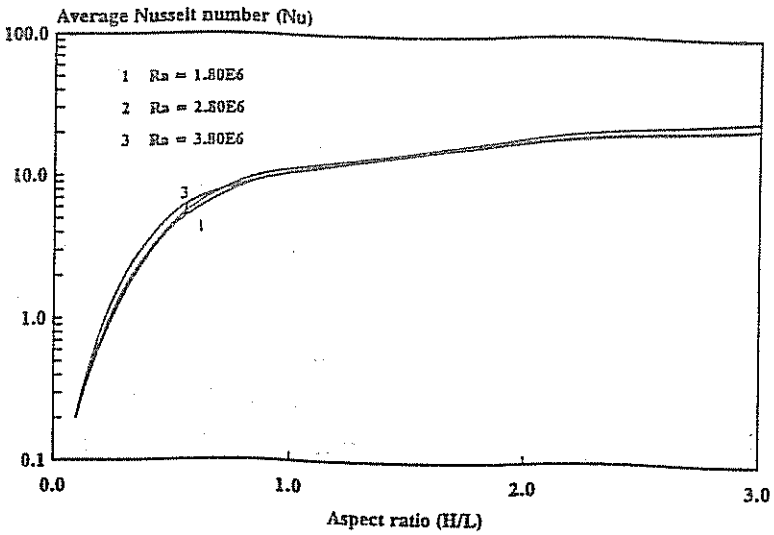

Fig. (16) Variation of the average Nusselt number with the aspect ratio for different Rayleigh numbers